Composites Science and Technology 123 (2016) 92–98

Contents lists available at ScienceDirect

Composites Science and Technology

journal homepage: http://www.elsevier.com/locate/compscitech

Microcombing enables high-performance carbon nanotube composites

Liwen Zhang [a], Xin Wang [a], Ru Li [b], Qingwen Li [b], Philip D. Bradford [c], Yuntian Zhu [a, *]

[a] Department of Materials Science and Engineering, North Carolina State University, Raleigh, NC, 27695, USA
[b] Suzhou Institute of Nano-Science and Nano-Biotics, Chinese Academy of Sciences, Suzhou, Jiangsu, 215123, China
[c] Department of Textile Engineering Chemistry and Science, North Carolina State University, Raleigh, NC, 27695, USA

ARTICLE INFO

Article history:
Received 1 August 2015
Received in revised form
12 December 2015
Accepted 16 December 2015
Available online 19 December 2015

Keywords:
Carbon nanotubes
Polymer-matrix composites (PMCs)
Electrical properties
Mechanical properties
Microcombing

ABSTRACT

A processing approach, microcombing, has been reported recently to produce dry carbon nanotube (CNT) films with superior mechanical and electrical properties by taking advantage of its efficiency in straightening the wavy CNTs and aligning the strands. Here, we report the fabrication of CNT composite films with aligned CNTs and CNT strands, reduced waviness, high CNT weight fraction, and relatively uniform CNT distribution, using poly(vinyl alcohol) (PVA) as a model matrix. These structural features give the micro-combed CNT/PVA composite films electrical conductivity of 1.84×10^5 S/m, Young's modulus of 119 GPa, tensile strength of 2.9 GPa, and toughness of 52.4 J/cm^3, which improve over those of uncombed samples by 300%, 100%, 120%, and 200%, respectively, and are also much higher than those obtained by other processing approaches. Moreover, this method is expected to be applicable to various polymer matrices as long as they can be dissolved in the solution.

1. Introduction

Carbon nanotubes (CNTs) possess remarkable mechanical [1,2] and electrical properties [3]. In combination with their low density and high aspect ratio, CNTs are ideal candidates as advanced reinforcements for nanocomposites, which offer tremendous opportunities for developing multifunctional materials, such as structural composites, transparent electrodes, energy storage devices, field and thermionic emission electron sources [4–7]. For decades, CNT/polymer composites have been the focus of scientific research. Various techniques have been explored to achieve organized CNT structures with superior performance, from short-CNT-reinforced polymer fibers [8–10] to long and aligned CNT/polymer composite films [11,12], from solution-based methods [13–17] to dry-processable approaches [18–24].

CNTs have one-dimensional tube structures with unidirectional mechanical, electrical, and thermal properties. Therefore, it is of great importance to control their orientation and configurations when assembling them into macroscopic composites [5,25]. Studies have shown that the excellent intrinsic properties of CNTs can be better utilized when unidirectionally-aligned long nanotubes are assembled in a composite structure with a high CNT fraction [7,16,18,19], and nanotube waviness is a critical factor that limits the overall performance of CNT composites [20,23,26].

Recently, our group reported a novel approach known as "microcombing" to fabricate dry, pure CNT films (without any matrix) by utilizing unidirectionally-aligned long nanotubes [27]. By passing a single layer of CNT sheet through micro-scale rough edges of surgical blades, the microcombing process straightened wavy CNTs, reduced the impurities in the film structure, and increased the film packing density and uniformity, which in turn greatly improved the properties of the assembled CNT films. The method is simple and reliable to fabricate CNT films with reproducible properties. However, the greatly improved CNT straightness and packing density may cause another issue – strand agglomeration – in the films, which causes problems when this kind of CNTs are used to produce CNT/polymer composites. It is believed that the high performance CNT/polymer composites require the CNTs to be well dispersed in order to achieve a good interfacial load transfer with the polymer matrix [13,14]. This casts doubt on if the microcombing method can be used to fabricate high performance CNT/polymer composites. This is an issue that we need to address, otherwise our method will only have limited applications.

In this study, we incorporated our microcombing method into a one-step winding approach [20] to fabricate CNT/polymer

* Corresponding author.
E-mail address: ytzhu@ncsu.edu (Y. Zhu).

http://dx.doi.org/10.1016/j.compscitech.2015.12.012
0266-3538/

composites. A layered composite structure was designed as it could maintain the aligned structure of nanotubes, realize high CNT loading, and ensure intimate interaction between the matrix and nanotubes, all of which promoted load transfer [28,29]. PVA was used as a model matrix in our study to represent other soluble polymer matrices, because it has great processability and excellent adhesive property, and has been widely used to enhance the strength of CNT yarns and films [16–19,21,30]. Moreover, PVA is biocompatible and nontoxic. The CNT/PVA yarns and films can be made into fabrics which show potential applications in spacesuits, bullet-proof vests, and radiation protection suits. In addition, they are promising materials for bioapplications [18,31].

It is found that the as-produced micro-combed CNT/PVA composite films are strong (2.9 GPa) and stiff (119 GPa), which are much higher than other reported values for CNT/PVA composite yarns and sheets. They also exhibit a high toughness of 52.4 J/cm^3 and a high electrical conductivity of 1.84×10^5 S/m at a high CNT weight fraction of ~75%. Moreover, this method is simple, reliable, and reproducible, which provides for a new way to produce high performance CNT/polymer composites at large scale and low cost, while a wide range of soluble polymer matrices can be utilized.

2. Experimental

2.1. Growth of CNT arrays

The drawable CNT arrays used in this study were synthesized using a chemical vapor deposition method, as described in our previous work [22]. Briefly, electron-beam evaporation technique was used first to prepare the catalyst by depositing an alumina layer (20 nm) and an iron layer (1 nm) on a silicon substrate with thermal oxide (30 nm). Then, this substrate was put in a 5-inch quartz tube to grow CNT array at 740 °C. A gas mixture of argon with 6% hydrogen and pure ethylene were used for CNT growth. The total flow rate of gases was set at 1.5 L/min. After growing for 15 min, the array was approximately 200 μm in height. Most nanotubes have 2–5 walls and are 4–8 nm in diameters (Fig. 1).

2.2. Preparation of the polymer solution

PVA (MW = 75,000–80,000, ≥99.0% hydrolyzed) was purchased from Sinopharm Chemical Reagent Co., Ltd. The PVA solution used in the experiment had a concentration of 0.1 wt.%, which was found to be optimal in our previous study [19]. The solution was prepared by dissolving PVA into equal volume of deionized water and ethanol.

2.3. Fabrication of the micro-combed CNT/PVA composite films

The experimental setup of microcombing for making the CNT/PVA composite films is shown in Fig. 2. The microcombing zone consisted of a pair of sharp surgical blades, which were positioned oppositely. A layer of CNT sheet was drawn from a drawable CNT array, and then went through the microcombing zone. The contact angle between the CNT sheet and the blade was controlled at 80°~85°, and the inter-blade distance was set at about 6 cm (Fig. 2b). In the microcombing zone, micro-scale rough edges of the surgical blades acted as combs that straightens the wavy CNTs and provides better CNT alignment. A rotating mandrel with a diameter of 3 cm was used to wind the CNT sheet into macroscopic film at a rotational speed of 20 r/min. The PVA matrix was applied on the CNT sheet layer-by-layer using a needle. And another needle was bent into 90° and placed at 1 o'clock position of the rotating mandrel. The needles had a diameter of 0.65 mm. The bent-needle contacted the surface of the mandrel so that a little pressure from the needle's weight was applied to the CNT sheet. The PVA solution was applied in between the mandrel and the bent-needle at a rate of about 0.3 g/min. In this way, the bent-needle surface helped to spread the matrix more uniformly compared with only the drop-process [20].

Two hundred revolutions produced a film with a thickness of about 4 μm. The CNT film was then peeled off from the mandrel and hot-pressed under a pressure of 10 MPa at 80 °C for 2 h followed by 160 °C for another 2 h in order to remove air bubbles and improve CNT-polymer integration. The hot-pressing reduced film thickness

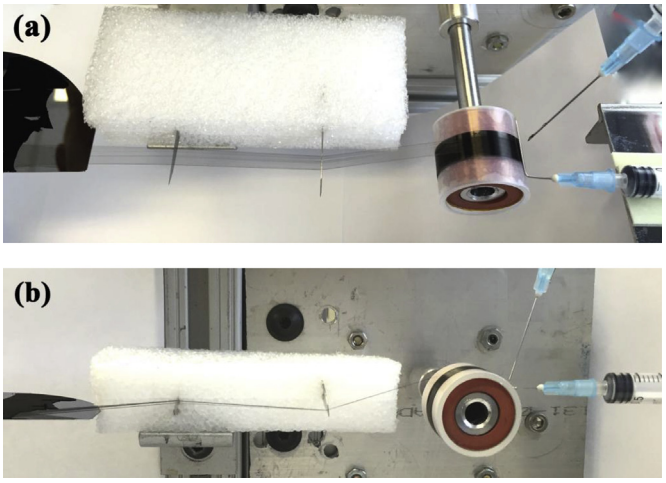

Fig. 2. Experimental setup of the one-step approach of making CNT/polymer composite films.

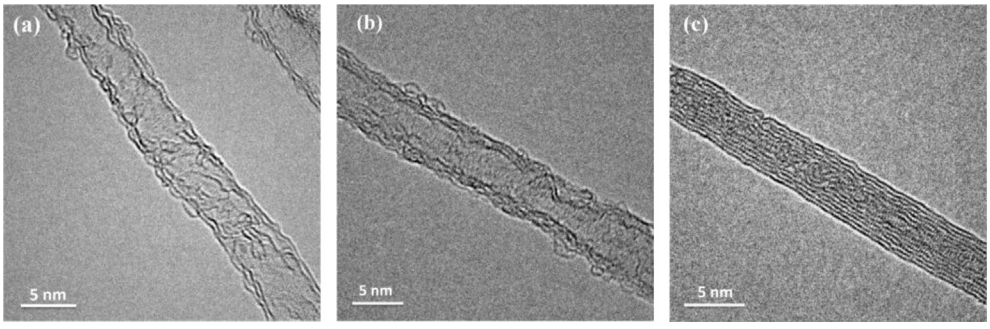

Fig. 1. TEM images showing the diameter and number of walls of individual CNT.

to about 3 μm.

For comparison, CNT/PVA composite films without microcombing were produced using the same parameters.

2.4. Characterization methods

Transmission electron microscopy (TEM, JEOL-2010F) analysis was conducted at 200 kV to reveal the diameter and number of walls of individual nanotubes. The CNT alignment was studied by both scanning electron microscopy (SEM, Verios 460L) and X-ray diffraction (XRD). Azimuthal scans of the XRD measurements were performed using Rigaku SmartLab with Eulerian cradle equipped with Cu rotating anode (Kα wavelength of 1.5418 Å). Each pattern was measured using a step size of 1° and a scan rate of 1°/s at $2\theta = 23.5°$. The fracture surface morphology of the as-produced films was also analyzed by SEM. Weight fractions of the CNT composites were determined by thermogravimetric analysis (TGA, Perkin Elmer Pyris 1) in nitrogen (99.999%) at a heating rate of 10 °C/min.

A 4-probe Agilent 34410A 6.5 digit multimeter was used to test the electrical conductivity of the films along the CNT alignment direction. Electrodes were made of silver by magnetron sputtering. Tensile test specimens were prepared by cutting the as-produced films into narrow strips, which were typically 1 mm wide and 10 mm in gauge length. The width of the specimen was measured using a calibrated scale bar in an optical micrometer. The thickness was measured by a micrometer and further confirmed by SEM. The specimens were tested in tension by an Instron 3365 tensile testing machine using a load cell of 10 N and a displacement rate of 0.5 mm/min. In order to calculate the film density, the weight of each specimen was measured using a MX5 microbalance (Mettler-Toledo, Inc.), which had an accuracy of 1 μg.

3. Results and discussion

3.1. Morphologies of the uncombed and combed CNT/PVA composite films

Fig. 3 presents SEM images showing both the surface morphologies and the fracture surfaces of uncombed and combed CNT/PVA composite films. As shown, microcombing produced CNT/PVA composite films with straighter CNTs, improved alignment, enhanced nanotube packing, and increased film uniformity, which was consistent with the results from our previous study on dry CNT films [27]. The CNT alignment can also be characterized by the anisotropic angular distribution intensity of the (002) reflection,

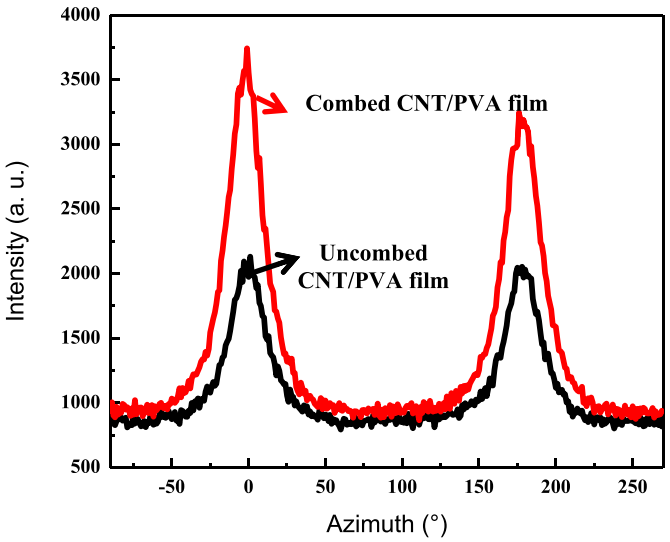

Fig. 4. The integrated X-ray intensity of the (002) reflection along the 2θ axis versus the azimuth (ϕ) before and after microcombing.

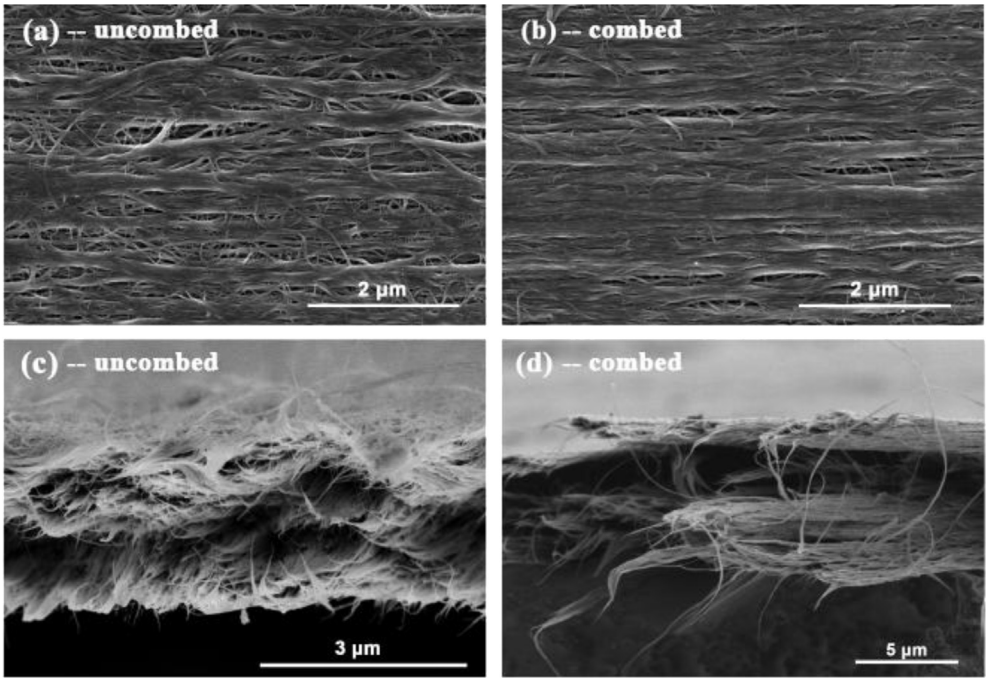

Fig. 3. SEM images showing the differences of surface morphologies and the fracture surfaces between the uncombed and combed CNT/PVA films.

which is related to the inter-wall distance of nanotubes [32–34]. A non-uniform (002) intensity indicates the CNTs are aligned. Fig. 4 shows the integrated X-ray intensity of the (002) reflection along the 2θ axis versus the azimuth (ϕ). Two peaks are centered at $\phi \approx -1^{\circ}$ and 178°, respectively, indicating a preferred orientation of nanotubes. The full width at half-maximum (FWHM) of the uncombed films is approximately 25°, while that of the combed films is about 23°, demonstrating an improved alignment of the CNTs by microcombing [32].

The CNT-polymer interaction is an essential factor that affects the efficiency of load transfer across the CNT-polymer interface [30]. Traditional infiltration method usually involves a densely-packed CNT film infiltrated with polymer matrix, where the nanotubes are not uniformly distributed in the matrix [12]. The "spray-winding" approach enables the polymer to be infiltrated into each layer of the CNT sheet with a more uniform CNT distribution [19,21,23]. However, the airflow generated by the sprayer usually disturbs the CNT alignment in the as-wound CNT sheet. The matrix-applying method used in the microcombing approach avoided this issue by applying polymer matrix using the smooth surface of a needle (Fig. 2). This method allowed CNTs to interact with the PVA matrix at molecular level with higher CNT-matrix contact area than that produced by the "spray-winding" approach, leading to more effective load transfer. As shown in Fig. 3 (c) & (d), the as-produced composite films exhibited a layered structure with PVA matrix homogeneously wrapping the CNT strands. The combed films showed a more severe strand agglomeration than the uncombed ones, since the CNTs were straighter and packed denser. In addition, the combed composites exhibited reduced defects along the axial direction of the composites, thus they were more likely to be torn apart instead of fracturing during tensile deformation (Fig. 5). The delamination was more severe for the combed films than the uncombed ones, suggesting the formation of strong CNT strands by microcombing. Therefore, it has been a challenge to take SEM images of the fracture surfaces of the combed CNT/PVA composite films. The as-produced CNT/PVA composite films had a high CNT weight fraction of ~75%, as calculated from the TGA results (Fig. 6), which helped to enhance the mechanical properties of the composites.

3.2. Electrical properties

The electrical conductivities of the uncombed and combed CNT/PVA composite films are shown in Fig. 7 (also Table S1 in the supplementary material), and they are compared with the values reported for the uncombed and combed dry CNT films [27]. Microcombing increased the electrical conductivity of the CNT/PVA films by 300% from 0.45×10^5 S/m to 1.84×10^5 S/m, which was to our knowledge higher than any other reported values for CNT/PVA composite yarns and films [18,19,21]. This improvement could be accredited to the enhanced nanotube alignment, straightness, and packing by microcombing (Fig. 3), which resulted in increased inter-tube contact area for more efficient electron transfer [35,36]. The enhanced packing could be inferred from the increased film density: 0.86 g/cm^3 for uncombed CNT/PVA composite films, and

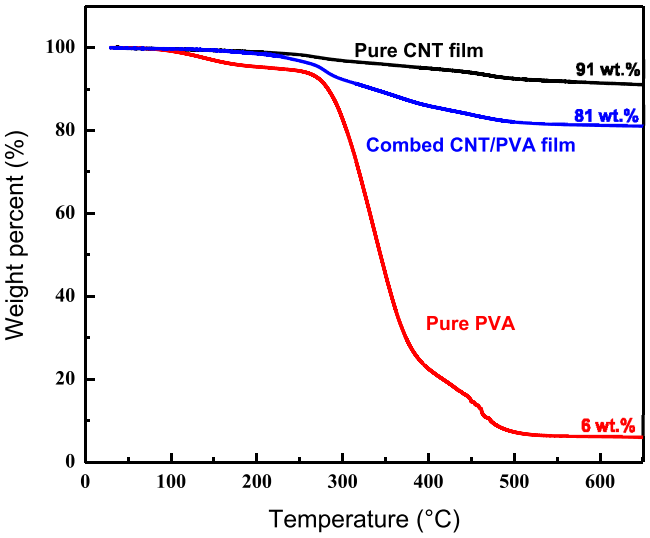

Fig. 6. TGA curves of pure CNT film, a combed CNT/PVA composite film, and pure PVA.

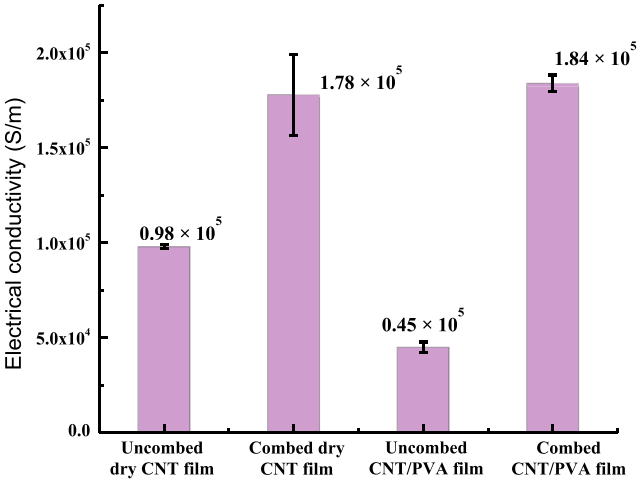

Fig. 7. Electrical conductivity of the CNT/PVA composite films in comparison with that of the dry CNT films.

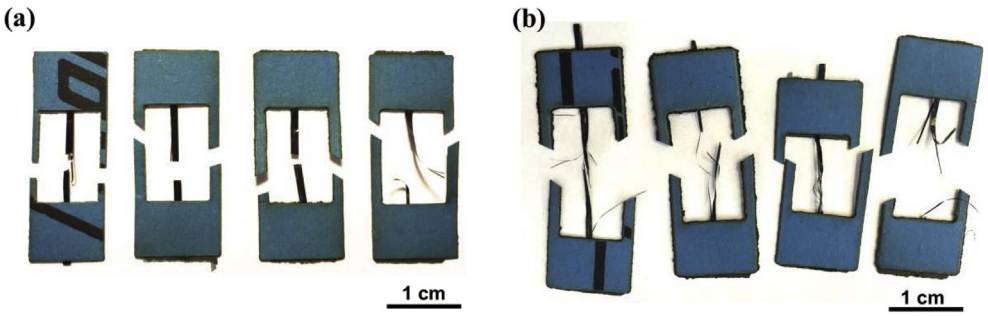

Fig. 5. Photos showing the fracture of the uncombed (a) and combed (b) CNT/PVA films.

Table 1
Summary of mechanical properties of the as-produced uncombed and combed CNT/PVA composite films.

Film type	Density (g/cm^3)	Young's modulus (GPa)	Tensile strength (GPa)	Strain (%)	Toughness (J/cm^3)
Uncombed CNT/PVA films	0.86	60 ± 4	1.3 ± 0.04	2.7 ± 0.2	17.4 ± 1.8
Combed CNT/PVA films	0.96	119 ± 6	2.9 ± 0.2	3.1 ± 0.2	52.4 ± 5.2
Improvement	12%	100%	120%	15%	200%

0.96 g/cm^3 for combed ones (Table 1).

Interestingly, the incorporation of the insulating PVA matrix decreased the average electrical conductivity of the uncombed films, but did not decrease the conductivity of the combed films. In particular, the combed CNT/PVA composite films showed 3.4% (6×10^3 S/m) higher average electrical conductivity than the combed dry CNT films. This phenomenon was also found in the reported work of CNT/PVA yarns and films [18,19]. Since electron transfer was largely controlled by the contact area between the nanotubes, the wrapping of the insulating PVA around the CNTs generated an insulating barrier which decreased the inter-tube contact area, leading to a decreased electrical conductivity of the uncombed CNT/PVA films. In comparison, when the CNTs were combed and had a closer inter-tube distance, CNT strand agglomeration occurred and the PVA molecules were hardly able to penetrate into those highly packed strands. Instead, the PVA matrix might have helped wrap the strands together, maintaining the close contact of the individual nanotubes against each other. In the combed dry CNT films, the film structure was loose and the contacts between the CNTs were not stable. Therefore, the combed dry CNT films showed slightly lower average electrical conductivity than the combed CNT/PVA films, but larger standard deviation. In this case, CNT strand agglomeration caused by microcombing did not impair the electrical properties of the as-produced composites, but it helped the electron transfer instead.

3.3. Mechanical properties

The mechanical properties of the uncombed and combed CNT/PVA composite films are summarized in Table 1. Fig. 8 displays their typical stress–strain curves. The Young's modulus (60 GPa) and tensile strength (1.3 GPa) of the uncombed composite films were comparable to the reported values of the CNT/PVA films made of the same CNTs [19]. After microcombing, the films' Young's modulus showed about 100% improvement to 119 GPa, and their tensile strength showed about 120% improvement to 2.9 GPa, which were quite significant. Compared to our dry CNT films reported previously (Young's modulus: 172 GPa, tensile strength: 3.2 GPa) [27], the Young's modulus and tensile strength both decreased after adding the PVA matrix. However, the total tensile load of the composite film was actually higher than that of the dry film with similar CNT quantity, but the addition of the matrix increased the thickness of the samples, which in turn resulted in reduced values of Young's modulus and tensile strength, which were normalized by the film thickness. In other words, the lower Young's modulus was caused by lower CNT volume fraction in the CNT/PVA composite sample than in the dry pure CNT films if the void space was taken as matrix in the latter. Moreover, the PVA was a thermal plastic that could act as lubricant between the CNT strands, which inevitably made the composite films less stiff during deformation. Therefore, the Young's modulus showed a larger degree of decrease than the tensile strength. The mechanical properties of the combed CNT/PVA films were much higher than those reported for CNT/PVA films and yarns [18,19]. Microcombing straightened the wavy CNTs, and packed them denser and more uniformly, which improved their mechanical properties.

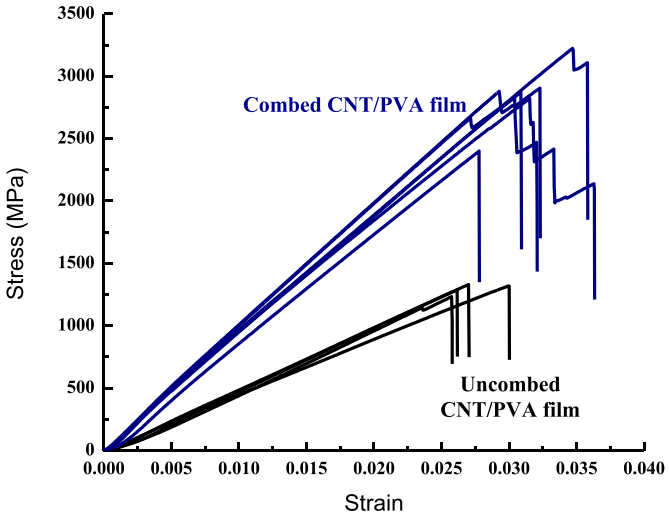

Fig. 8. Typical stress–strain curves of the uncombed and combed CNT/PVA films.

Examination of Fig. 8 also revealed a few interesting phenomena. First, the stress–strain curves of the combed CNT/PVA composites were serrated before failure. In other words, the total stress, which was calculated as the total load divided by the initial cross-sectional area of the sample, had several abrupt drops and slow rises before the final failure. In contrast, no such obvious serrations were on the stress–strain curves of the uncombed CNT/PVA sample. This phenomenon was apparently caused by the successive fracture of individual large CNT strands in the combed sample. When a large CNT strand was broken, the load carried by the strand was suddenly reduced to zero, which caused an abrupt large drop in the total load carried by the sample. This led to an abrupt drop in the apparent stress in the stress–strain curve. The stress continued to increase slowly as the remaining CNT strands were strained further. The above process might repeat itself a few times before the final failure of the composite sample. Such a large abrupt load drop could only be caused by the fracture of large CNT strands. The fracture of individual CNTs or small CNT strands would not lead to observable stress drops because they did not carry high enough load individually. The uncombed CNT/PVA composite samples did not show such serrated stress–strain curves, indicating that no large CNT strands were formed in the sample. This is another evidence on the promotion of large CNT strands by microcombing, which is consistent with the aforementioned big increase in electrical conductivity by microcombing.

Second, the strains to failure of the CNT/PVA films were larger after microcombing (Fig. 8), which suggested that during tensile deformation, combed CNTs were more likely to slide against each other than to break. The enhanced tensile strength and strain significantly increased the film toughness by 200% from 17.4 J/cm^3 to 52.4 J/cm^3 (Table 1). This is another consequence of formation of large CNT strands promoted by microcombing. Any future studies on the micro-combed CNT composites should take into account this structural feature.

The simplicity of the microcombing also makes properties of our

composites reproducible, which is of great importance since reproducibility has been a challenge in CNT composites fabrication. For several samples we have made, the mechanical behavior of both the uncombed and the combed CNT/PVA composite films are in good consistency, as shown in Fig. 8. Based on our further studies, which is to be reported in the future, the microcombing approach can be used to make CNT composite with any polymer matrix if the matrix can be dissolved in a solvent to form a dilute polymer solution. It would be interesting to see how the mechanical properties are affected if a stiffer and stronger polymer matrix such as epoxy is used to make micro-combed CNT composite.

It should be noted that this method needs to use high-quality drawable CNT array, which is more difficult to produce in large quantity than CNT powder. On the other hand, CNT powders have so far failed to produce high-strength composites because of their intrinsic limitations in dispersion, length, alignment and volume fraction.

4. Conclusions

In this study, it is demonstrated that our recently developed microcombing method can also be used to produce high performance CNT/polymer composite films. By using PVA as a model matrix, we successfully fabricated the CNT/PVA composite films with superior electrical and mechanical properties. The microcombing method provided straightened CNTs, enhanced packing density, and reduced impurities in the composites. The microcombing promoted the formation of CNT strands, but this was found beneficial for enhancing the composite performance. The as-produced CNT/PVA composite films exhibit an electrical conductivity of 1.84×10^5 S/m, Young's modulus of 119 GPa, tensile strength of 2.9 GPa, and toughness of 52.4 J/cm^3, which represent improvements over those of uncombed samples by 300%, 100%, 120%, and 200%, respectively. While this method is simple, reliable, and reproducible, it is also expected to be applicable to a variety of soluble polymers. In addition, since PVA is a thermal plastic polymer that has relatively low mechanical properties compared with thermoset polymers, we believe that our microcombing method can produce CNT/polymer composites with even better properties if high performance matrix is used.

Acknowledgments

The authors thank Suzhou Institute of Nano-Science and Nano-Biotics for collaboration. The authors acknowledge the use of the Analytical Instrumentation Facility (AIF) at North Carolina State University, which is supported by the State of North Carolina and the National Science Foundation. This work was funded by the US Air Force Office of Scientific Research (Grant No. FA9550-12-1-0088).

Appendix A. Supplementary data

Supplementary data related to this article can be found at http://dx.doi.org/10.1016/j.compscitech.2015.12.012.

References

[1] M.F. Yu, O. Lourie, M.J. Dyer, K. Moloni, T.F. Kelly, R.S. Ruoff, Strength and breaking mechanism of multiwalled carbon nanotubes under tensile load, Science 287 (2000) 637–640, http://dx.doi.org/10.1126/science.287.5453.637.
[2] M.F. Yu, B.S. Files, S. Arepalli, R.S. Ruoff, Tensile loading of ropes of single-wall carbon nanotubes and their mechanical properties, Phys. Rev. Lett. 84 (2000) 5552–5555, http://dx.doi.org/10.1103/PhysRevLett.84.5552.
[3] T.W. Ebbesen, H.J. Lezec, H. Hiura, J.W. Bennett, H.F. Ghaemi, T. Thio, Electrical conductivity of individual carbon nanotubes, Nature 382 (1996) 54–56, http://dx.doi.org/10.1038/382054a0.
[4] R.H. Baughman, A.A. Zakhidov, W.A. de Heer, Carbon nanotubes–the route toward applications, Science 297 (2002) 787–792, http://dx.doi.org/10.1126/science.1060928.
[5] L.Q. Liu, W.J. Ma, Z. Zhang, Macroscopic carbon nanotube assemblies: preparation, properties, and potential applications, Small 7 (2011) 1504–1520, http://dx.doi.org/10.1002/smll.201002198.
[6] K.L. Jiang, J.P. Wang, Q.Q. Li, L.A. Liu, C.H. Liu, S.S. Fan, Superaligned carbon nanotube arrays, films, and yarns: a road to applications, Adv. Mater 23 (2011) 1154–1161, http://dx.doi.org/10.1002/adma.201003989.
[7] J.T. Di, X. Wang, Y.J. Xing, Y.Y. Zhang, X.H. Zhang, W.B. Lu, et al., Dry-processable carbon nanotubes for functional devices and composites, Small 10 (2014) 4606–4625, http://dx.doi.org/10.1002/smll.201401465.
[8] J.C. Kearns, R.L. Shambaugh, Polypropylene fibers reinforced with carbon nanotubes, J. Appl. Polym. Sci. 86 (2002) 2079–2084, http://dx.doi.org/10.1002/app.11160.
[9] J.K.W. Sandler, S. Pegel, M. Cadek, F. Gojny, M. van Es, J. Lohmar, et al., A comparative study of melt spun polyamide-12 fibres reinforced with carbon nanotubes and nanofibres, Polymer 45 (2004) 2001–2015, http://dx.doi.org/10.1016/j.polymer.2004.01.023.
[10] E.M. Moore, D.L. Ortiz, V.T. Marla, R.L. Shambaugh, B.P. Grady, Enhancing the strength of polypropylene fibers with carbon nanotubes, J. Appl. Polym. Sci. 93 (2004) 2926–2933, http://dx.doi.org/10.1002/app.20703.
[11] Q.F. Cheng, J.P. Wang, J.J. Wen, C.H. Liu, K.L. Jiang, Q.Q. Li, et al., Carbon nanotube/epoxy composites fabricated by resin transfer molding, Carbon 48 (2010) 260–266, http://dx.doi.org/10.1016/j.carbon.2009.09.014.
[12] P.D. Bradford, X. Wang, H.B. Zhao, J.P. Maria, Q.X. Jia, Y.T. Zhu, A novel approach to fabricate high volume fraction nanocomposites with long aligned carbon nanotubes, Compos. Sci. Technol. 70 (2010) 1980–1985, http://dx.doi.org/10.1016/j.compscitech.2010.07.020.
[13] X.F. Zhang, T. Liu, T.V. Sreekumar, S. Kumar, V.C. Moore, R.H. Hauge, et al., Poly(vinyl alcohol)/SWNT composite film, Nano Lett. 3 (2003) 1285–1288, http://dx.doi.org/10.1021/nl034336t.
[14] J.N. Coleman, M. Cadek, R. Blake, V. Nicolosi, K.P. Ryan, C. Belton, et al., High performance nanotube-reinforced plastics: understanding the mechanism of strength increase, Adv. Funct. Mater 14 (2004) 791–798, http://dx.doi.org/10.1002/adfm.200305200.
[15] K.P. Ryan, M. Cadek, V. Nicolosi, S. Walker, M. Ruether, A. Fonseca, et al., Multiwalled carbon nanotube nucleated crystallization and reinforcement in poly(vinyl alcohol) composites, Synth. Met. 156 (2006) 332–335, http://dx.doi.org/10.1016/j.synthmet.2005.12.015.
[16] Z. Wang, P. Ciselli, T. Peijs, The extraordinary reinforcing efficiency of single-walled carbon nanotubes in oriented poly(vinyl alcohol) tapes, Nanotechnology 18 (2007) 455709, http://dx.doi.org/10.1088/0957-4484/18/45/455709.
[17] Y.L. Zhu, Z.J. Du, H.Q. Li, C. Zhang, Preparation and crystallization behavior of multiwalled carbon nanotubes/poly(vinyl alcohol) nanocomposites, Polym. Eng. Sci. 51 (2011) 1770–1779, http://dx.doi.org/10.1002/pen.21964.
[18] K. Liu, Y.H. Sun, X.Y. Lin, R.F. Zhou, J.P. Wang, S.S. Fan, et al., Scratch-resistant, highly conductive, and high-strength carbon nanotube-based composite yarns, ACS Nano 4 (2010) 5827–5834, http://dx.doi.org/10.1021/nn1017318.
[19] W. Liu, X.H. Zhang, G. Xu, P.D. Bradford, X. Wang, H.B. Zhao, et al., Producing superior composites by winding carbon nanotubes onto a mandrel under a poly(vinyl alcohol) spray, Carbon 49 (2011) 4786–4791, http://dx.doi.org/10.1016/j.carbon.2011.06.089.
[20] X. Wang, P.D. Bradford, W. Liu, H.B. Zhao, Y. Inoue, J.-P. Maria, et al., Mechanical and electrical property improvement in CNT/Nylon composites through drawing and stretching, Compos. Sci. Technol. 71 (2011) 1677–1683, http://dx.doi.org/10.1016/j.compscitech.2011.07.023.
[21] W. Liu, H.B. Zhao, Y. Inoue, X. Wang, P.D. Bradford, H. Kim, et al., Poly(vinyl alcohol) reinforced with large-diameter carbon nanotubes via spray winding, Compos. Part Appl. Sci. Manuf. 43 (2012) 587–592, http://dx.doi.org/10.1016/j.compositesa.2011.12.029.
[22] J.T. Di, D.M. Hu, H.Y. Chen, Z.Z. Yong, M.H. Chen, Z.H. Feng, et al., Ultrastrong, foldable, and highly conductive carbon nanotube film, ACS Nano 6 (2012) 5457–5464, http://dx.doi.org/10.1021/nn301321j.
[23] X. Wang, Z.Z. Yong, Q.W. Li, P.D. Bradford, W. Liu, D.S. Tucker, et al., Ultrastrong, stiff and multifunctional carbon nanotube composites, Mater. Res. Lett. 1 (2013) 19–25, http://dx.doi.org/10.1080/21663831.2012.686586.
[24] X. Wang, Q. Jiang, W.Z. Xu, W. Cai, Y. Inoue, Y.T. Zhu, Effect of carbon nanotube length on thermal, electrical and mechanical properties of CNT/bismaleimide composites, Carbon 53 (2013) 145–152, http://dx.doi.org/10.1016/j.carbon.2012.10.041.
[25] M. Zhang, Strong, transparent, multifunctional, carbon nanotube sheets, Science 309 (2005) 1215–1219, http://dx.doi.org/10.1126/science.1115311.
[26] F. Fisher, Fiber waviness in nanotube-reinforced polymer composites—I: Modulus predictions using effective nanotube properties, Compos. Sci. Technol. 63 (2003) 1689–1703, http://dx.doi.org/10.1016/S0266-3538(03)00069-1.
[27] L.W. Zhang, X. Wang, W.Z. Xu, Y.Y. Zhang, Q.W. Li, P.D. Bradford, et al., Strong and Conductive Dry Carbon Nanotube Films by Microcombing, Small 11 (2015) 3830–3836, http://dx.doi.org/10.1002/smll.201500111.
[28] A.A. Mamedov, N.A. Kotov, M. Prato, D.M. Guldi, J.P. Wicksted, A. Hirsch, Molecular design of strong single-wall carbon nanotube/polyelectrolyte multilayer composites, Nat. Mater 1 (2002) 190–194, http://dx.doi.org/10.1038/nmat747.

[29] P. Podsiadlo, A.K. Kaushik, E.M. Arruda, A.M. Waas, B.S. Shim, J. Xu, et al., Ultrastrong and stiff layered polymer nanocomposites, Science 318 (2007) 80–83, http://dx.doi.org/10.1126/science.1143176.
[30] W.J. Ma, L.Q. Liu, Z. Zhang, R. Yang, G. Liu, T.H. Zhang, et al., High-strength composite fibers: realizing true potential of carbon nanotubes in polymer matrix through continuous reticulate architecture and molecular level couplings, Nano Lett. 9 (2009) 2855–2861, http://dx.doi.org/10.1021/nl901035v.
[31] N.Y. Zhang, J.N. Xie, V.K. Varadan, Soluble functionalized carbon nanotube/poly(vinyl alcohol) nanocomposite as the electrode for glucose sensing, Smart Mater. Struct. 15 (2006) 123–128, http://dx.doi.org/10.1088/0964-1726/15/1/040.
[32] L. Jin, C. Bower, O. Zhou, Alignment of carbon nanotubes in a polymer matrix by mechanical stretching, Appl. Phys. Lett. 73 (1998) 1197, http://dx.doi.org/10.1063/1.122125.
[33] M. Huard, F. Roussel, S. Rouzière, S. Patel, M. Pinault, M. Mayne-L'Hermite, et al., Vertically aligned carbon nanotube-based composite: Elaboration and monitoring of the nanotubes alignment, J. Appl. Polym. Sci. 131 (2014) 39730, http://dx.doi.org/10.1002/app.39730.
[34] S. Boncel, K.K.K. Koziol, K.Z. Walczak, A.H. Windle, M.S.P. Shaffer, Infiltration of highly aligned carbon nanotube arrays with molten polystyrene, Mater. Lett. 65 (2011) 2299–2303, http://dx.doi.org/10.1016/j.matlet.2011.04.065.
[35] J.M. Nugent, K.S.V. Santhanam, A. Rubio, P.M. Ajayan, Fast electron transfer kinetics on multiwalled carbon nanotube microbundle electrodes, Nano Lett. 1 (2001) 87–91, http://dx.doi.org/10.1021/nl005521z.
[36] J.E. Fischer, W. Zhou, J. Vavro, M.C. Llaguno, C. Guthy, R. Haggenmueller, et al., Magnetically aligned single wall carbon nanotube films: preferred orientation and anisotropic transport properties, J. Appl. Phys. 93 (2003) 2157, http://dx.doi.org/10.1063/1.1536733.